

Multinary metal alloys of the Heusler, half-Heusler, dilute magnetic semiconductors, and high entropy families: how would spin make a choice?

C. E. A. GRIGORESCU^{a,*}, C. N. ZOITA^a, A. SOBETKII^b, A.-M. IORDACHE^a, S.-M. IORDACHE^a, C. R. STEFAN^a, M. I. RUSU^a, L. TORTET^c, A. TONETTO^d, R. NOTONIER^c

^aNational Institute of R&D in Optoelectronics, INOE 2000, 409 Atomistilor, 077125, Magurele, Jud. Ilfov, Romania

^bMGM STAR Construct SRL-Bucharest, Romania,

^cMADIREL, Aix Marseille Universite, Marseille, France

^dPRATIM, Aix Marseille Universite, Marseille, France

Multinary alloys from the half-Heusler, Heusler, dilute magnetic semiconductors and magnetic high entropy alloys have been investigated for their properties to accommodate quantum spin states and touch Curie temperatures above room temperature as utterly desired for spintronic devices. Co, Mn and Fe are the core elements in the alloys studied here. High structural ordering has been found in Co-based Heusler alloys, followed by equiatomic high entropy alloys with close atomic radii also cobalt based. Curie points between 400 °C and 900 °C were found in all materials.

(Received November 26, 2020; accepted December 7, 2020)

Keywords: Spintronics, Half metals, Dilute magnetic semiconductors, Magnetic high entropy alloys, Heusler alloys

1. Introduction

Spintronics is an emerging field that exploits simultaneously the quantum spin states of electrons and their charge state. The electron spin manifests itself as a two state magnetic energy system. The “birth” of spintronics happened through the discovery of giant magnetoresistance in 1988 by Albert Fert, et al., and Peter Grünberg, et al., independently [1, 2]. Research in this field focuses mainly on the transport of spin-polarised electrons through the interface of two materials, thus leading to device applications. A simple model of a spin device-like structure would involve a ferromagnetic contact to inject polarised spin into a semiconductor through a tunnel barrier (insulator). The interest in integrating magnetoelectronic effects with semiconductor electronics to develop *spintronics* continues to be an area of growth and a topic of worldwide attention. Control and detection of spin order in ferromagnetic materials build the main principle that enables current technologies for storing and reading magnetic information. Recent theoretical and experimental research has been oriented to large spin injection efficiency and accumulated spin polarization including giant magnetoresistance, spin-torque and tunnel effects on electron transport. Thus, spin transport mechanisms can be described by two key features: the *spin polarization P*

$$P = \frac{n \uparrow - n \downarrow}{n \uparrow + n \downarrow} \quad (1)$$

that measures the imbalance in the density of electrons with opposite spins (leading to spin accumulation or depletion), and the *spin injection efficiency Γ* , which should be defined as the polarization of the injected current *J*:

$$\Gamma = \frac{J \uparrow - J \downarrow}{J \uparrow + J \downarrow} \quad (2)$$

The arrows \uparrow (\downarrow) denote the electron spin projection on a quantization axis. In ferromagnetic materials this is antiparallel to the magnetization moment *M*. The “spin relaxation time” is about 1 nsec and represents the duration of travelling of spin polarized electrons over macroscopic distances without losing polarization. These are details to be considered when designing alloys whose properties could lead to spin device applications. Interfaces between substrates/tunnel barriers and ferromagnetic alloy contacts are also critical elements.

There have been significant advances in understanding the technical challenges, particularly with respect to high spin injection efficiency between the spin polarised ferromagnet (SPFM) and the narrow gap semiconductors (NGS). A high interface resistance of a spin polarising tunnel barrier between the SPFM and NGS layers is an essential requirement. Concerning the ferromagnetic contacts, a special attention is devoted to materials with ferromagnetic ordering such as: Heusler Alloys (HAs), dilute magnetic semiconductors (DMSs), magnetic high entropy alloys (M-HEAs). DMSs that exhibit room temperature ferromagnetism have attracted lately an enormous interest through their unique capability of combining non-volatility and band gap

engineering in a single material [3]. An alloy is a phase containing two or more components. In a simple picture of binary alloys one component is seen as the solvent and the other one-as the solute. In principle, that could work for more components too. From the structure point of view, metal alloys are either ordered or disordered, crystalline, polycrystalline, or amorphous.

There are 3 types of ordered alloys: 1) *substitutional*: the solute substitutes the solvent in the crystal lattice without structural changes; 2) *interstitial*: the solute resides in crystallographic pores; 3) *transformational*: an entirely new lattice is built as a result of intermetallic compound formation. For example, mixing numerous 3d-elements and subsequently melting them together, or allowing them to undergo a solid-state reaction, give rise to random solid solutions with a high configurational entropy.

Properties of metals are mainly defined by their electron structure. This, and other aspects are summarised by Hume-Rothery rules that are taken into account when building substitutional solid solutions:

1. *Atomic Size Factor* (the 15% rule) - the relative difference between the atomic diameters (radii) of two species < 15% (>15% limited solubility);

2. *Crystal Structure*: an appreciable solid solubility exists when the crystal structures of elements are identical;

3. *Valency*: the solute and solvent atoms should typically have the same valence in order to achieve maximum solubility;

4. *Electronegativity difference close to 0 gives maximum solubility*.

The alloys HAs, DMS, and M-HEAs described here have been designed and prepared following Hume-Rothery rules as both bulk and thin film [4-6].

2. Experimental

For bulk growth we have used mainly the vertical gradient freeze technique (VGF). Thin films were produced by pulsed laser deposition (PLD). Investigations on structural properties have been carried out by X-ray diffraction (XRD), energy dispersive X-ray spectroscopy (EDX), and reflection high energy electron diffraction (RHEED), whereas morphology was observed by scanning electron microscopy (SEM). Curie points were measured by thermogravimetric analysis (TGA) in a magnetic field.

2.1. Heusler, half-Heusler and Dilute Magnetic Semiconductors

We have grown Ni_2MnSb , Co_2MnSi , Co_2MnGa , Co_2MnGe , Co_2MnAl , and NiMnSb (HAs and half-HAs) from the Heusler family of ferromagnets with formulae X_2YZ and XYZ . HAs crystallize in the L_{21} structure, whereas half-HAs are of the C_{1b} . Both structures consist of four interpenetrating sublattices. L_{21} structure is similar to the C_{1b} except the vacant site in the fourth sublattice, which is occupied by an X atom. The alloys with $\text{X} = \text{Co}$ and $\text{Y} = \text{Mn}$ are ferromagnets, carrying magnetic moments

on both Co and Mn atoms. Concerning the magnetic properties of these compounds, it is to underline that the manganese atom carries the largest magnetic moment (around $3 \mu_B$), whereas cobalt has only a moment of about $1 \mu_B$, and the Z atom is slightly antiferromagnetically spin-polarized with respect to Mn and Co [3]. When the Z elements are either Si or Ge, band structure calculations predict half-metallic behaviour [8, 9].

Ferromagnets or fully spin-polarised metals (half-metals) have usually high Curie temperature (T_C) e.g. $\text{Co}_2\text{MnSi} \sim 1000 \text{ K}$, which is one of the excellent characteristics for thin film magnetic sensor elements. These full Heusler alloys have attracted a lot of attention due to the diverse magnetic phenomena they exhibit. The most striking is the transition from a ferromagnetic phase to an antiferromagnetic one by changing the concentration of the carriers [9]. Other Z elements in the Co_2MnZ Heusler system, like for instance Ga and Sn, would provide interesting magnetic properties, but lack the half-metallicity. The half-metallic behaviour and their high Curie temperatures make the Co-based Heusler alloys extremely attractive for spin device applications operating at room temperature. It is to remark that almost all the known half-metallic ferromagnets are manganese-based compounds. One exception is CrO_2 . It occurs that cobalt gives a high stability to the ferromagnetic alignment in Co_2MnZ compounds, which is reflected in the high experimental Curie temperatures of 985 K, 905 K, and 829 K, in Co_2MnSi , Co_2MnGe , and Co_2MnSn , respectively [10, 11].

Crystallographic ordering in these compounds is essential to meet the spin polarization condition. However, bulk multicomponent alloys with homogeneous composition and desired crystallographic order are not straightforward to grow at large batches. Thin film deposition techniques, such as magnetron sputtering (MS), molecular beam epitaxy (MBE) and PLD are mostly used to make semiconductor/ferromagnetic half-metal structures [3, 12-14]. The choice is made according to cost-effectiveness, stoichiometry matters, and reproducibility of the processes. These criteria apply to any of the multicomponent alloys investigated here. Bulk Co_2MnSi , Co_2MnGe , Co_2MnSn in the range of stoichiometric Heusler compounds as well as non-stoichiometric Heuslers $\text{Co}_2\text{MnSb}_x\text{Sn}_{1-x}$ for $x=0.2; 0.6$, which are predicted to be half-metals, have been grown by the VGF technique.

We have deposited highly crystalline Co_2MnZ ($\text{Z}=\text{Si}, \text{Ge}, \text{Sn}, \text{Sb}_{0.8}\text{Sn}_{0.2}$) films having 30-400 nm thick onto Si, GaAs, InAs substrates [3] by PLD at moderate growth temperature ($T \leq 473 \text{ K}$). The stoichiometries correspond to those of the targets (EDX measurements, not shown here). In terms of droplets density, it was observed (SEM) that the lower the fluence the lower the number of droplets. The influence of the substrate on the Heusler film quality has been investigated by structural, optical, and magneto-optical measurements. For example, the lattice match between Co_2MnSi and GaAs made the corresponding film smoother and better ordered than films grown on mismatched substrates. Values of the lattice

parameters of various Co-based alloys, and their Curie temperatures, are shown in the Table 1.

Table 1. Lattice parameter and Curie temperature of some bulk Co-based Has

COMPOUND (nominal composition)	LATTICE PARAMETER		T_c [K]	
	Our work	Theory	Our work	Other works
Co ₂ MnSi	5.673(5)	5.606 [7]	996	985 [10, 15, 16]
Co ₂ MnGe	5.753(2)	5.711 [7]	883	905 [10, 15, 16]
Co ₂ MnGa	5.775(3)	5.677 [7]	688	694 [10, 15, 16]
Co ₂ MnSn	5.9943	5.982 [7]	850	829 [10, 15, 16]
Co ₂ MnSb _{0.2} Sn _{0.8}	5.9828	-	845	-
Co ₂ MnSb _{0.4} Sn _{0.6}	5.9653	-	773	-
Co ₂ MnSb _{0.6} Sn _{0.4}	5.9539	-	700	-
Co ₂ MnSb _{0.8} Sn _{0.2}	5.940(5)	-	645	-

The choice of a suitable substrate for spin device applications would start with this information [15-17].

Also, one should bare in mind the alternative offered by tunnel barriers. Sputtering and PLD assure most suitable kinetic energy levels of 1 ~ 10 eV that are ideal for alloy deposition [18].

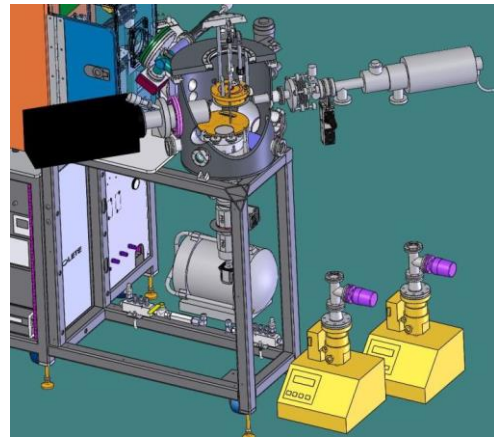
The easiest, and least expensive, way to achieve stoichiometric multicomponent films is through PLD, where stoichiometry of the target is transferred to the film. This has been tested with HAs, half-HAs, DMS, and HEAs using a PLD 2000 Workstation (PVD Products Ltd.) – Fig.1, with a 248 nm excimer laser [4].



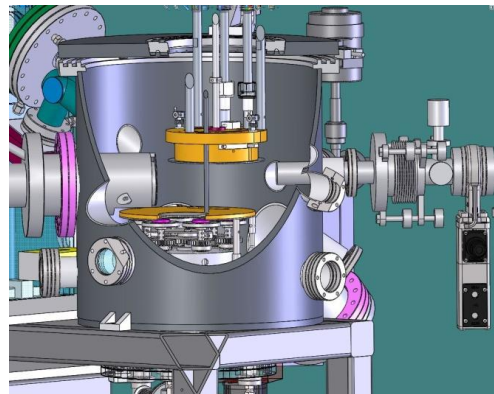
Fig. 1. PLD 2000 Workstation (PVD Products Ltd.), using 193 nm and 248 nm lasers (color online)

Ordering in the film structure critically depends on the substrate temperature during growth and not in the least of

the film–substrate lattice mismatch. A good insight into the surface structure, and film-substrate interface, can be gained by RHEED.



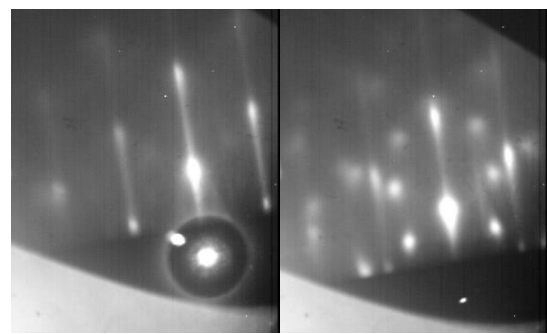
(a)



(b)

Fig. 2. (a) Schematic of the RHEED Gun, k-Space camera box and two HiPace turbo pumps; (b) close up of RHEED gun and screen inside deposition chamber (color online)

The RHEED system in Fig. 2 (PVD Products Ltd.) includes the ability to adjust both the incidence and azimuthal angle of the electron beam for proper alignment on the substrate surface. Thus, mechanical alignment is not needed.



(a)

(b)

Fig. 3. RHEED images along the (a) [110] and (b) [1-10] azimuths of a 54 nm DMS MnGe_{2.12}Sb_{1.04}:Co film grown at $T_{sub} = 200$ °C. Surface roughening and the appearance of stray phases are observed

In Fig. 3 and Fig. 4 are shown RHEED images of PLD thin films deposited from the DMS $\text{MnGe}_{2.12}\text{Sb}_{1.04}\text{Co}$ [4] on GaAs and HAs Co_2MnSi on Si.

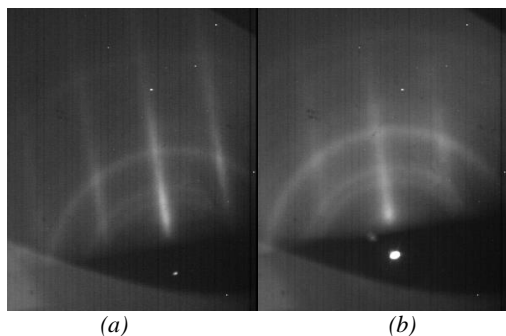


Fig. 4. RHEED images along the (a) $[110]$ and (b) $[1-10]$ azimuths of a 80 nm Co_2MnSi film grown at $T_{\text{sub}} = 100^\circ\text{C}$. There are not reconstruction streaks visible and stronger rings indicate a polycrystalline or amorphous component.

Clear DMS properties of $\text{MnGe}_{2.12}\text{Sb}_{1.04}\text{Co}$ PLD films have been demonstrated: ferromagnetic, with Curie point above 600 K, and a semiconductor like structure confirmed by mixed Drude and intraband contributions, as measured by spectral reflectivity between 0.6 and 6 eV [4]. However, the disordered structure of this material (see also Fig.3) is not expected yet to allow for spintronic applications.

2.2. Magnetic High Entropy Alloys

In the last decade, the interest for ferromagnetic films has been focused on increasing the number of elements from 2 to 3, 4, and more. High entropy alloys (HEAs) are composed of at least four to five principal elements in concentrations of 5–35 at. % [19, 20]. HEAs form solid-solutions that would build on structures like L_{21} , C_{1b} , or a combination of those [21]. Theoretical Curie temperatures maps have been elaborated to create ferromagnetic HEAs with desired Curie points and magnetizations [22], based on transition metals such as Co, Fe, Ni, Cr. Applications are sought for future magnetic refrigeration. Spin devices have been not yet predicted, although in particular alloys the spin-orbital coupling could be interrogated. This is a matter of electron structure and of crystallographic order. We have prepared two particular alloys with ferromagnetic properties and T_C above room temperature. Alloys with equiatomic ratios have the highest configurational entropy contribution to the free energy. However, the local or long range atomic order in HEAs remains unclear [21].

In this work we consider M-HEAs with strict equiatomic composition of principal elements with close atomic radii: (1) FeCoNiGeCu ; (2) TiAlCoNiGeCu . This is quite a challenge for magnetic alloys applications. Titanium and aluminium have been included for mechanical properties purposes. We applied Hume-Rothery rules to prepare bulk material for PLD targets. High-purity powders of Fe, Co, Ni, Ge, Cu, Ti, Al (Alfa Aesar) have been weighted in stoichiometric amounts

corresponding to each of the mentioned above alloys followed by milling together (Pulverisette 6-Fritsch), pressing into pellets, and annealing for 60 min to 1000°C in argon. HEA mixtures were melted in cylindrical alumina crucibles (Alfa Aesar). The temperature raised from RT to $T = T_{M(1;2)} + 30^\circ\text{C}$ at a rate of $20^\circ\text{C}/\text{min}$, then the melt was held 180 min at $T_M + 30^\circ\text{C}$ followed by cooling down to RT through adjusting the thermal gradient according to the composition. $T_{M(1;2)}$ are the melting points of the two alloys. Ingots 25 mm in diameter and 30 mm long have resulted, which were cut and polished. Investigations on structure, composition, and magnetic properties were run through (XRD)-Fig.5, (EDX)-Fig.6, and TGA in a magnetic field Fig.7. The XRD patterns show a combination of FCC and BCC structures in both alloys. Uniform composition has been found by EDX-mapping of all sides of the slices, although here we show only one example. TGA was performed in argon gas from RT to 1000°C and setting a 0.5 T permanent magnet underneath the Pt crucible.

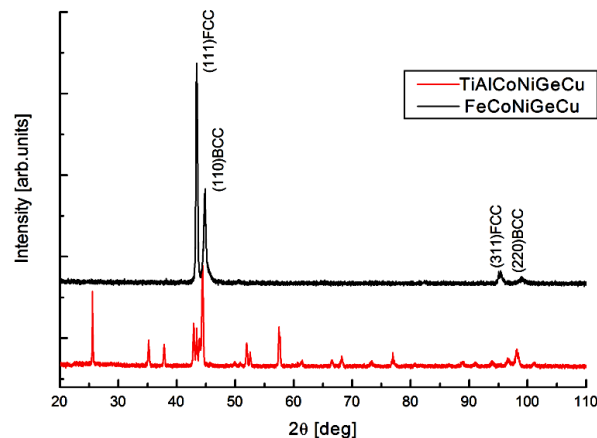


Fig. 5. XRD patterns of the two M-HEAs (color online)

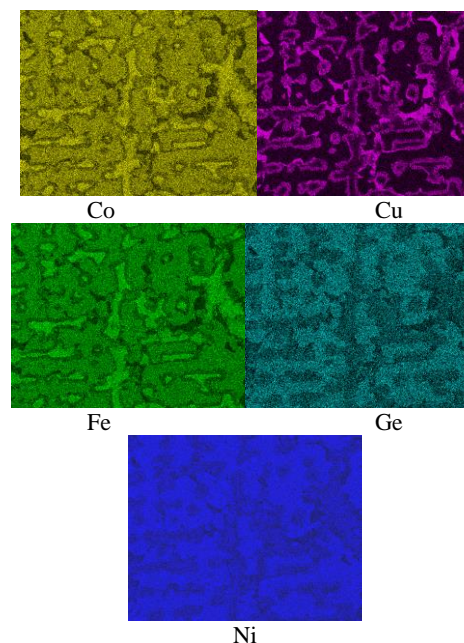


Fig. 6. EDX maps of the CoFeNiGeCu HEA (color online)

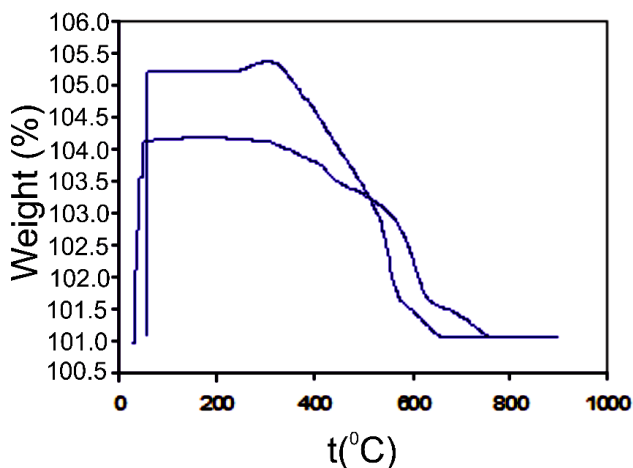


Fig. 7. TGA of the two alloys in a magnetic field. T_c are sensibly above room temperature

The Curie points of the two investigated M-HEAs are well above room temperature.

3. Conclusion

Various types of multinary alloys exhibit interesting magnetic properties when ordering can be achieved.

Hume-Rothery rules are extremely helpful in the synthesis of those alloys. Although ferromagnetism and semiconductor-like behaviour have been demonstrated in DMS $\text{MnGe}_{2.12}\text{Sb}_{1.04}\text{Co}$ the alloy exhibits too much disorder for spintronic applications.

HEAs with strict equi-atomic composition of principal elements with close atomic radii including Co and Fe look very promising in spintronics as magnetic contacts especially when high Curie temperatures are achieved. We have not investigated yet in the depth their intimate structural order and density of states. Cobalt based alloys from the Heusler family are still the friendliest to the spin travel through appropriate interfaces. Spin would make than choice of highly ordered materials.

Acknowledgements

This work was supported by a grant of the Romanian Ministry of Education and Research, CNCS - UEFISCDI, project number PN-III-P1-1.1-PD-2019-1134, within PNCDI III, CORE Programme, Ctr. 18/N/2019, Contract nr.19PFE/17.10.2018 financed by Ministry of Research and Innovation, M.ERANET-6059-TriboHEA UEFISCDI Programme 3, grant no. 113/2019.

The RHEED equipment used for surface characterisation of DMS $\text{MnGe}_{2.12}\text{Sb}_{1.04}\text{Co}$ and Heusler Co_2MnSi films was acquired by the infrastructure project INOVA-OPTIMA SMIS code 49164, contract no. 658/2014.

References

- [1] M. N. Baibich, J. M. Broto, A. Fert, F. Nguyen Van Dau, F. Petroff, P. Etienne, G. Creuzet, A. Friederich, J. Chazelas, *Phys. Rev. Lett.* **61**(21), 2472 (1988).
- [2] P. Grunberg, R. Schreiber, Y. Pang, M. B. Brodsky, H. Sowers, *Phys. Rev. Lett.* **57**(19), 2442 (1986).
- [3] M. I. Rusu, R. Savastru, D. Savastru, D. Tenciu, C. R. Iordanescu, I. D. Feraru, C. N. Zoita, R. Notonier, A. Tonetto, C. Chassigneux, O. Monnereau, L. Tortet, C. E. A. Grigorescu, *Appl. Surf. Sci.* **284**, 950 (2013).
- [4] M. Acet, *AIP Adv.* **9**(9), 095037 (2019)
- [5] S. Guo, C. Ng, J. Lu, C. T. Liu, *J. Appl. Phys.* **109**(10), 103505 (2011).
- [6] S.-M. Na, P. K. Lambert, H. Kim, J. Paglione, N. J. Jones, *AIP Adv.* **9**(3), 035010 (2019)
- [7] S. Ishida, S. Fujii, S. Kashiwagi, S. Asano, *J. Phys. Soc. Jpn.* **64**(6), 2152 (1995).
- [8] S. Picozzi, A. Continenza, A. J. Freeman, *Phys. Rev. B* **66**(9), 094421 (2002).
- [9] S. Skaftouros, K. Özdoğan, E. Şaşıoğlu, I. Galanakis, *Appl. Phys. Lett.* **102**(2), 022402 (2013).
- [10] J. Kubler, A. R. Williams, C. B. Sommers, *Phys. Rev. B* **28**(4), 1745 (1983).
- [11] M. Kawakami, Y. Kasamatsu, H. Ido, *J. Magn. Magn. Mater.* **70**(1-3), 265 (1987).
- [12] C. Vitelaru, I. Pana, A. E. Kiss, N. C. Zoita, A. Vladescu, M. Braic, *J. Optoelectron. Adv. M.* **21**(11-12), 717 (2019).
- [13] S. Mican, D. Benea, A. Takacs, E. Mossang, O. Isnard, V. Pop, *J. Optoelectron. Adv. M.* **21**(5-6), 407 (2019).
- [14] Y. Wang, Y. Liu, Q. Zhai, M. Zhang, *Optoelectron. Adv. Mater.* **12**(9-10), 579 (2018).
- [15] W. Van Roy, P. Van Dorpe, V. Motsnyi, Z. Liu, G. Borghs, Jo De Boeck, *Phys. Status Solidi B Basic Res.* **241**(7), 1470 (2004).
- [16] X. Y. Dong, C. Adelman, J. Q. Xie, C. J. Palmstrom, X. Lou, J. Strand, P. A. Crowell, J.-P. Barnes, A. K. Petford-Long, *Appl. Phys. Lett.* **86**(10), 102107 (2005)
- [17] A. S. Manea, O. Monnereau, R. Notonier, F. Guinneton, C. Logofatu, L. Tortet, A. Garnier, M. Mitrea, C. Negrila, W. Branford, C. E. A. Grigorescu, *J. Cryst. Growth* **275**(1-2), e1787 (2005).
- [18] E. Y. Vedmedenko R. K. Kawakami, D. D. Sheka, P. Gambardella, A. Kirilyuk, A. Hirohata, C. Binek, O. Chubykalo-Fesenko, S. Sanvito, B. J. Kirby, J. Grollier, K. Everschor-Sitte, T. Kampfrath, C.-Y. You, A. Berger, *J. Phys. D* **53**(45), 453001 (2020).
- [19] J.-W. Yeh, S.-K. Chen, S.-J. Lin, J.-Y. Gan, T.-S. Chin, T.-T. Shun, C.-H. Tsau, S.-Y. Chang, *Adv. Eng. Mater.* **6**(5), 299 (2004).
- [20] B. Cantor, I. T. H. Chang, P. Knight, A. J. B. Vincent, *Mater. Sci. Eng. A* **375–377**, 213 (2004).

[21] C. Niu, A. J. Zaddach, A. A. Oni, X. Sang, J. W. Hurt III, J. M. LeBeau, C. C. Koch, D. L. Irving, *Appl. Phys. Lett.* **106**(16), 161906 (2015).

[22] F. Kormann, D. Ma, D. D. Belyea, M. S. Lucas, C. W. Miller, B. Grabowski, M. H. F. Sluiter, *Appl. Phys. Lett.* **107**(14), 142404 (2015).

*Corresponding author: krisis812@yahoo.co.uk